International Journal of Thermophysics, Vol. 11, No. 1, 1990

Dual-Wavelength Radiation Thermometry: Emissivity Compensation Algorithms[1]

B. K. Tsai,[2] R. L. Shoemaker,[2] D. P. DeWitt,[2] B. A. Cowans,[3] Z. Dardas,[3] W. N. Delgass,[3] and G. J. Dail[4]

The traditional contact methods of temperature measurement for metal processing applications provide accuracies of ± 10 K. Noncontact methods based upon emissivity compensation techniques have the potential for improved accuracy with greater ease of use but require prior knowledge of the target emissivity behavior. The features of the basic spectral and ratio methods and five dual-wavelength methods are reviewed. Experiments were conducted on a series of aluminum alloys with different surface treatments characterized by x-ray photoelectron spectroscopy in the temperature range 600 to 750 K. Compensation algorithms that account for surface characteristics are required to achieve improved accuracy.

KEY WORDS: dual-wavelength radiation thermometry; emissivity; pyrometry; radiation thermometry; radiometry; surface characterization; temperature measurement; x-ray photoelectron spectroscopy.

1. INTRODUCTION

Accurately measuring the temperature of aluminum alloys during processing is a challenging problem. The commonly used contact methods employ two-pronged thermocouples or other contact devices which can achieve accuracies of ± 10 K but are difficult to use. Direct noncontact or radiometric methods have the potential for increased accuracy and ease of use but necessitate some knowledge of the spectral emissivity of the target

[1] Paper presented at the Tenth Symposium on Thermophysical Properties, June 20–23, 1988, Gaithersburg, Maryland, U.S.A.

[2] School of Mechanical Engineering, Purdue University, West Lafayette, Indiana 47907, U.S.A.

[3] School of Chemical Engineering, Purdue University, West Lafayette, Indiana 47907, U.S.A.

[4] Lafayette Works, Aluminum Company of America, Lafayette, Indiana, U.S.A.

0195-928X/90/0100-0269$06.00/0

material. Spectral emissivity data are difficult to acquire since the emissivity of aluminum alloy surfaces depends on many variables, including temperature, wavelength, surface conditions, process conditions, and thermal history. Further, the inherently low emissivity and high reflectivity of aluminum alloy surfaces make property measurements difficult under laboratory or simulated mill conditions. In addition, environmental factors in the mill, such as vibrations and electrical noise, contribute greatly to the complexity of radiometric design necessary to make reliable observations. These problems emphasize the difficulty of achieving reliable temperature measurements for automatic control and metallurgical quality requirements, increasing product reproducibility and reliability, and reducing cost [1].

In applying any radiation thermometry method, some assumptions must be made on the emissivity of the target material. The spectral method, the simplest and most widely used approach, requires that the target have a constant and known emissivity. The ratio method, which requires approximately gray surfaces, finds special utility with highly oxidized metallics and nonmetallics but does not work well with low-emissivity metals. These methods can be satisfactorily used for numerous applications where the errors due to emissivity uncertainties are known and acceptable. Foley [2] has demonstrated a modified ratio method which allows for nongray behavior. The cross-correlation method of Svet [3] had good accuracy with near-black surfaces (cavities) experiencing small emissivity changes. The method of Watari et al. [4, 5] employed an algorithm involving emissivity as an exponential function of wavelength with oxidized stainless steels. Anderson [6, 7] used a linear combination of the ratio and spectral radiance temperatures for low-emissivity metallic surfaces.

The adjustable parameters of these dual-wavelength methods have not been related to surface conditions, and hence, the methods have found limited utility. An understanding of the effect of changing surface conditions on emissivity is essential in identifying the proper emissivity function or compensation algorithm. Because of the attractions of simplified, mill-hardened instrumentation, there are strong incentives to investigate whether dual-wavelength methodology, with appropriate algorithms, can satisfy an accuracy of ± 3 K for aluminum alloy processes. The objectives of the study are (1) to review dual-wavelength emissivity compensation algorithms, (2) to evaluate the effectiveness of these algorithms in predicting the true temperature of aluminum surfaces using laboratory data, and (3) to examine surface conditions for a relationship between emissivity and surface microstructure.

2. PRINCIPLES OF THE METHODS

Dual-wavelength radiation thermometry is based upon two relations which are written below for a spectral condition. Because our interest is generally restricted to wavelengths shorter than the peak of the blackbody curve, Wien's law

$$L_{\lambda,\mathrm{b}} = \frac{c_1 \lambda^{-5}}{\exp(c_2/\lambda T)} \tag{1}$$

is a good approximation to Planck's law for the spectral radiance distribution. The spectral emissivity can be expressed as the ratio of the blackbody spectral radiance at the spectral radiance temperature (T_λ) to the blackbody spectral radiance at the true temperature (T),

$$\varepsilon_\lambda = \frac{L_{\lambda,\mathrm{b}}(\lambda, T_\lambda)}{L_{\lambda,\mathrm{b}}(\lambda, T)}. \tag{2}$$

From these relations, the *spectral temperature equation* is

$$\frac{1}{T} = \frac{1}{T_\lambda} + \frac{\lambda}{c_2} \ln \varepsilon_\lambda \tag{(3)}$$

In the *spectral* method, the true temperature is inferred by measurement of the spectral temperature, T_λ, and knowledge of the spectral emissivity, ε_λ, at a specified wavelength.

For the *ratio* method, using the same basic relationships, but written for two spectral conditions, the *ratio temperature equation* is

$$\frac{1}{T} = \frac{1}{T_\mathrm{r}} + \frac{\Lambda_\mathrm{r}}{c_2} \ln\left(\frac{\varepsilon_1}{\varepsilon_2}\right) \tag{4}$$

where the ratio temperature, T_r, and the equivalent wavelength, Λ_r, are defined such that

$$\frac{1}{T_\mathrm{r}} = \Lambda_\mathrm{r}\left[\frac{1}{\lambda_1 T_{\lambda 1}} - \frac{1}{\lambda_2 T_{\lambda 2}}\right] \tag{5}$$

$$\Lambda_\mathrm{r} = \frac{\lambda_1 \lambda_2}{\lambda_2 - \lambda_1} \tag{6}$$

To achieve emissivity compensation, the second term on the right-hand side of Eq. (4) needs to be zero or a known constant independent of temperature and surface conditions; that is, the ratio method requires that

$$\frac{\varepsilon_1}{\varepsilon_2} = \text{constant} \tag{7}$$

The *Foley* method [2] (FOL) is a variation of the ratio method and has a temperature equation of the form

$$\frac{1}{T}=\frac{1}{T_{\mathrm{mr}}}+\frac{\Lambda_{\mathrm{r}}}{c_2}\left[(1-K_{\mathrm{f}}\lambda_1)\ln\varepsilon_1-(1-K_{\mathrm{f}}\lambda_2)\ln\varepsilon_2\right] \tag{8}$$

where T_{mr} is the modified-ratio temperature defined by

$$\frac{1}{T_{\mathrm{mr}}}=\Lambda_{\mathrm{r}}\left[\frac{1-K_{\mathrm{f}}\lambda_1}{\lambda_1 T_{\lambda 1}}-\frac{1-K_{\mathrm{f}}\lambda_2}{\lambda_2 T_{\lambda 2}}\right] \tag{9}$$

Emissivity compensation is achieved when the term in paren theses in Eq. (8) is zero, namely,

$$\frac{\ln\varepsilon_1}{\ln\varepsilon_2}=\frac{1-K_{\mathrm{f}}\lambda_2}{1-K_{\mathrm{f}}\lambda_1} \tag{10}$$

where K_{f} is the parameter which is adjusted to account for nongray behavior. Note that when $K_{\mathrm{f}}=0$, T_{mr} becomes the ratio temperature (T_{r}) and the FOL method reduces to the *ratio temperature equation*, Eq. (4).

The *Watari* method [4, 5] (WAT) is yet another variation of the ratio method and has a temperature equation of the form

$$\frac{1}{T}=\frac{A}{T_{\lambda 1}}+\frac{B}{T_{\lambda 2}} \tag{11}$$

where

$$A=\frac{1}{1-(\lambda_1/\lambda_2)^3},\qquad B=\frac{1}{1-(\lambda_2/\lambda_1)^3}. \tag{12, 13}$$

That is, the reciprocal of the temperature is a specified linear combination of the two spectral radiance temperatures. Alternatively the temperature equation can be written as

$$\frac{1}{T}=\frac{1}{T_{\mathrm{r}}}+\frac{\Lambda_{\mathrm{r}}}{c_2}\alpha(\lambda_1^2-\lambda_2^2) \tag{14}$$

from which it is evident that the emissivity compensation algorithm has the form

$$\varepsilon_\lambda=\exp(\alpha\lambda^2) \tag{15}$$

The preceding temperature equations have their origins in simply prescribed emissivity functions, Eqs. (7), (10), and (15). An alternative

approach is to postulate empirical forms of the temperature equations. The *ratio-with-offset* method (RWO) is a variation of the ratio method and relates the true temperature to the ratio temperature plus a constant offset.

$$T = T_r + B \tag{16}$$

This relationship is commonly used in commercial ratio instruments, and emissivity compensation is achieved if B is a known constant.

Anderson [6, 7] recognized that for metallic surfaces the spectral radiance and ratio temperatures are systematically lower and higher, respectively, than the true temperature. He postulated an empirical temperature equation of the form

$$T = (1 - x_0) T_r + x_0 T_{\lambda 2} \tag{17}$$

referred to as the *linear spectral-ratio* (LSR) method, in which the true temperature (T) is expressed as a linear combination of the ratio temperature (T_r) and a spectral temperature ($T_{\lambda 2}$). It can be shown that x_0 is related to emissivity by

$$\frac{\ln \varepsilon_1}{\ln \varepsilon_2} = 1 - \frac{x_0}{1 - x_0} \frac{\lambda_2}{\Lambda_r} \left(1 - \frac{\Lambda_r T}{c_2} \ln \frac{\varepsilon_1}{\varepsilon_2}\right) \Big/ \left(1 - \frac{\lambda_2 T}{c_2} \ln \varepsilon_2\right) \tag{18}$$

A variation of this approach, referred to as the *inverse spectral-ratio* (ISR) method, uses reciprocal temperatures, giving

$$\frac{1}{T} = \frac{(1 - y_0)}{T_r} + \frac{y_0}{T_{\lambda 2}} \tag{19}$$

for which the parameter y_0 can be expressed as

$$\frac{\ln \varepsilon_1}{\ln \varepsilon_2} = 1 - \frac{y_0}{1 - y_0} \frac{\lambda_2}{\Lambda_r} \tag{20}$$

By comparing Eqs. (10) and (20), it is evident that the emissivity compensation requirements of the FOL and ISR methods are identical. The LSR method contains a parameter x_0, which is dependent upon T, but for short-wavelength and low-temperature conditions, the LSR method compensates for emissivity in approximately the same manner as the ISR method.

3. EXPERIMENTAL APPARATUS AND PROCEDURES

An apparatus was developed to observe both the spectral radiance and the true temperatures of aluminum alloy samples. Its main functions

included calilbration of the radiometer against a reference blackbody, measurement of spectral radiances from the sample, control and measurement of sample temperature, and computation of spectral radiance temperatures. The experimental arrangement included a two-band radiometer (Williamson,[5] modified Model 12200, $2.1 \pm 0.05\ \mu m$, $2.4 \pm 0.05\ \mu m$) calibrated against a blackbody (Williamson, Model 45), a gold mirror which allowed sighting either the blackbody or the sample, a 10-channel digital thermometer (Fluke, Model 2176A), an interface for amplification and integration of radiometer signals, and a microcomputer (Zenith, Model ZW-248-82). The samples were heated by two embedded electrical heating elements, which were powered by a digital temperature controller (Watlow, Model 808C-0100-0000). The *true* surface temperature of the sample was determined from a thermocouple positioned parallel to and at a depth of 1.6 mm from the surface. A heat transfer analysis of the heater-sample arrangement showed the sample temperature to be uniform within $\pm 0.25°C$ [9]. At the start of each experiment, the radiometer was calibrated against the blackbody in the range of 550–750 K, and a linear regression of spectral radiance vs signal output for both spectral bandpasses was obtained. Following completion of the planned heating schedule, the regression result was checked against the true temperature to confirm satisfactory radiometer performance.

Radiometric measurements were made on four types of aluminum alloys (1100, 2224, 5052, 7075) with different surface conditions (C, as cast; E, as extruded; P, as polished; S, as cut). Cast samples were cut from the surface of an ingot that had left a direct chill casting mold. Extruded samples was passed through an extrusion die and had surfaces with a degree of roughness in the range of 0.1 to 0.5 μm. Polished surfaces were defined as the condition obtained by standard metallurgical polishing procedures ending with 800 grit Al_2O_3. Saw-cut samples were made by a circular cutoff saw resulting in a directional surface with rms roughnesses ranging from 4 to 12 and 0.15 to 2.4 μm across and along the sawing direction.

Three sets of experimental data were examined. The first set was comprised of the results from seven samples (1100E, 1100S, 5052E, 5052S, 7075C, 7075E, 7075S) at temperatures in the range of 620–760 K and heating times of 7–62 h. No special effort was made to expose these alloy samples systematically to similar heating schedules. The second data set was taken on the 1100E, 1100S, 5052E, and 5052S alloys and was measured at a fixed temperature of 740 K. Two different samples of the 5052E alloy were used with short (1-h) and long (4-h) heating exposures but for the other three

[5] The mention of a commercial product is provided for completeness of description of the experimental procedure but does not constitute an endorsement.

alloys only one sample of each alloy was used. The third data set, also at 740 K, included observations on the 2224P and 2224S alloys, each with long-term (4.5-h) and short-term (1-h) heating schedules. Attention was given to these samples to assure similarity in heating schedules, temperatures, etc.

The spectral emissivities were calculated from Eq. (2), while the *inferred* temperatures, as well as the parameters, for the LSR, ISR, and the RWO methods were evaluated using a least-squares technique, in which the sum of the squares of the temperature errors, the true minus the inferred temperature, $(T - T_{inf})$, was minimized. The first data set was also analyzed with the FOL and WAT algorithms. The *true* temperature was determined from thermocouple observations.

Angle-resolved x-ray photoelectron spectroscopy, ARXPS, provided information on the composition of the metal surface and the oxidation states of the elements present. Spectra were collected on the 1100, 2224, and 5052 alloys and recorded on a Perkin–Elmer PHI 5300 spectrometer. The Mg (1253.6 eV)/Al (1486.6 eV) dual-anode x-ray source was operated at 15 kV and 300 or 400 W, respectively. The spectrometer was calibrated by setting the binding energies of the Au $4f_{7/2}$ and Cu $2p_{3/2}$ levels to 84.0 and 932.7 eV, respectively. The full width at half-maximum for the Ag $3d_{5/2}$ level (368.4 eV) was 0.86 eV at 489 kHz for the pass energy at which data were collected. Background pressure in the analysis chamber was always less than 1×10^{-9} Torr. Data accumulation times to measure major and minor species at a given angle were roughly 16 h, and data reduction was accomplished using Perkin–Elmer software.

4. DISCUSSION

The results of the first data set in Fig. 1 indicated that the ISR method was identical to the FOL method as expected from the earlier discussion. In addition, the ISR method was moderately more accurate than the LSR method. For the types of alloys used and the temperature range selected, the WAT method proved to be the last accurate. For the full range of temperature from 620 to 740 K, the best precision with any method was ± 10 K. The results for the extruded samples displayed a temperature error $(T - T_{inf})$ that increased with temperature, whereas the temperature error associated with either the cast or saw-cut samples decreased with temperature. This phenomenon may be linked to the emissivity ratio behaviors of the types of samples because, as the emissivity ratio increases, the inferred temperature (T_{inf}) increases and the temperature error $(T - T_{inf})$ decreases in the RWO, LSR, and ISR methods. More data and analysis would be necessary to substantiate this statement clearly. The least-squares

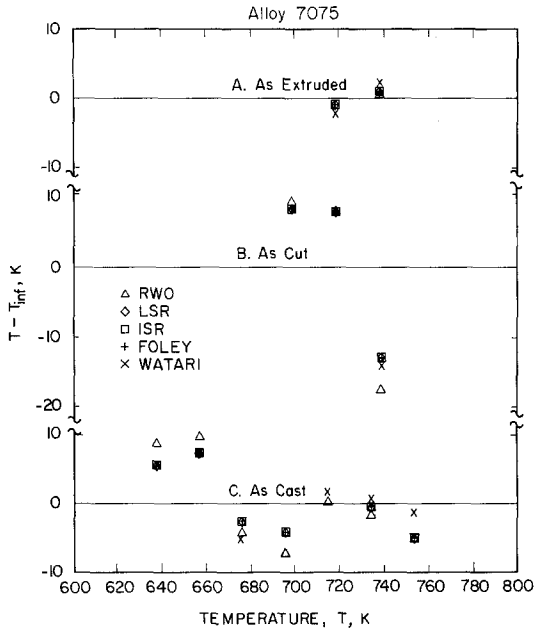

Fig. 1. Difference between true temperature and inferred temperature, $T - T_{inf}$, using the five emissivity compensation methods for the aluminum alloy 7075 under the (A) as-extruded, (B) as-cut, and (C) as-cast conditions.

analysis revealed that the RWO method was the best method for extruded samples, while the ISR and the FOL methods were most appropriate for the cast and saw-cut samples.

The second data set, shown in Fig. 2, revealed that the emissivity of the 1100 series alloys remained constant throughout the 5-h heating schedule, while the emissivity of the 5052S and 505E alloys doubled in the same time interval. Note that the sample-to-sample variation was approximately 0.02. As expected from surface roughness effects, the emissivity of the 1100S alloy was consistently higher than that of the 1100E alloy. The emissivity of the 5052S alloy was higher than that of the 1100 series alloys and increased with time as did the 5052E alloy. Again, the accuracy of the emissivity compensation methods was not better than ± 10 K.

The third set of results showed that the emissivity of the 2224S and 2224P alloys exposed to long-term (Fig. 3) and short-term heating schedules increased only slightly with time. In addition, the emissivity of

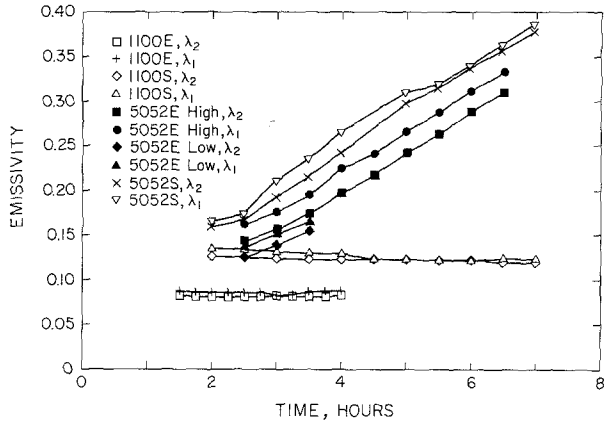

Fig. 2. Emissivity at 740 K for the aluminum alloys 1100 and 5052 under the saw-cut and extruded conditions.

the polished surfaces was less than the emissivity of the saw-cut surfaces. The accuracy of the compensation methods was not better than ± 10 K.

In the temperature difference or compensation results (Fig. 1) and the emissivity determinations (Fig. 2), the major sources of measurement error were due to uncertainties in observed spectral radiances, in radiometer calibration, and in the target temperature. The radiometer calibration uncertainty at the lower spectral radiance temperatures (about 600 K) was unacceptably large. Above 600 K, the error in temperature difference was

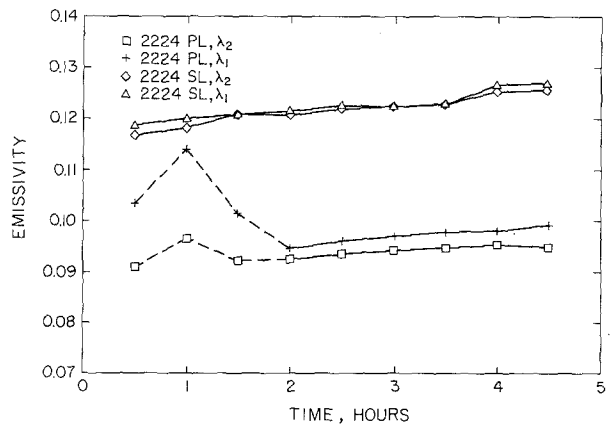

Fig. 3. Emissivity at 740 K for the aluminum alloy 2224 under the saw-cut and polished conditions with long-term heating.

about ± 5 K for the full range of temperatures. The differences among the methods were not altered by this random error, because the results were derived from the same set of experimental data. The error band for the temperature difference calculations is ± 5 K, while the error band for the emissivity determinations is about ± 0.005.

The ARXPS results were analyzed to provide a measure of the oxide layer thickness and composition. The oxide layer thickness was calculated from the relative intensities of the Al 2p lines for the Al and Al_2O_3 states as shown in Fig. 4. If we assume a uniform oxide layer of thickness covering an infinitely thick metal substrate, the equation relating the relative intensities has the form

$$\frac{I_{Al_2O_3}}{I_{Al}} = \frac{S_{Al_2O_3}\sigma_{Al_2O_3}\eta_{Al_2O_3}\lambda_{Al_2O_3}[1-\exp(-d/\lambda_{Al_2O_3}\sin\Theta)]}{S_{Al}\sigma_{Al}\eta_{Al}\lambda_{Al}\exp(-d/\lambda_{Al}\sin\Theta)} \tag{21}$$

where I is the intensity, S is the spectrometer term, which includes the analyzer transmission function, the detector efficiency, etc., σ is the photoelectron cross section [10], η is the atomic density, λ is the photoelectron mean free path [11], and Θ is the angle between the sample surface and the electron path to the analyzer. Since the Al and Al_2O_3 lines are very close in energy, we assume that the spectrometer terms are equal and solve Eq. (21) for the oxide layer thickness, d. The results of these calculations are shown in Fig. 5 and are discussed below. Note that the maximum thickness measurable by this method for this system is approximately 15 nm.

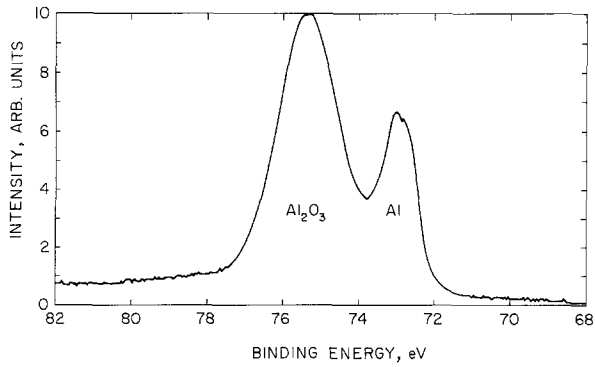

Fig. 4. X-ray photoelectron spectrum of the Al(2p) core level from 2224E at an electron takeoff angle of 60°. The two peaks show the chemical shift of Al_2O_3 from Al. An increase in the intensity ratio of $I_{Al_2O_3}/I_{Al}$ at a lower electron takeoff angle (spectrum not shown) confirms that the Al_2O_3 layer lies above the unoxidized aluminum.

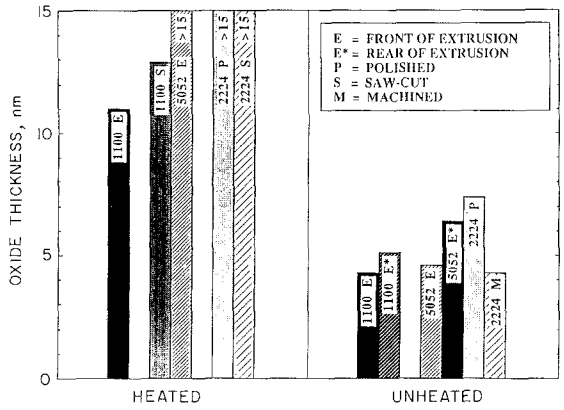

Fig. 5. Oxide layer thickness as determined by ARXPS for various alloys and conditions.

The fresh 1100E alloy possessed a relatively thin Al_2O_3 layer of roughly 4 to 5 nm. Prior to heating the sample, the oxide layer was slightly enriched in MgO relative to the nominal bulk Mg concentration. This result was also observed on the 2224 and 5052 alloys. Heating the 1100E alloy for 7 h at 740 K produced an Al_2O_3 layer approximately 11 nm thick with a MgO layer less than one monolayer thick. Note that the oxide thickness for the 1100S sample is 12.9 nm. The emissivity of this alloy remained constant at 740 K, as shown in Fig. 2.

Both machined (M) and polished (P) surfaces of the 2224 alloy were examined. The machined surface had an Al_2O_3 layer of 4.3-nm thickness and was similar in composition to the 1100 alloy, while the polished surface had an oxide layer 7.4 nm thick that was righ in Mg. The effect of polishing on oxide thickness has been noted previously [12]. The 2224 alloy, which contains slightly less Mg but much more Cu than the 5052 alloy, produced a MgO layer approximately 15 nm thick when heated to 740 K for only 1 h. Although some Al_2O_3 could be observed, the total oxide thickness of this alloy became too thick to measure with ARXPS. Extended heating for 4.5 h did not appear to increase the thickness of the MgO layer significantly. Thus, heating the 2224 alloy produces a surface oxide layer which is MgO for the first 15 nm and Al_2O_3 for an unspecified depth below the MgO. The emissivity of this alloy increased slightly over a 4.5-h period.

The oxide thickness of the unheated 5052E alloy changed from 4.6 to 6.4 nm from the front to the rear of the extrusion. Further, the surface at the rear of the extrusion contained nearly three times the amount of MgO as the front of the extrusion. When heated for 1 h at 740 K, the 5052 alloy produced a MgO layer greater than the 15-nm limit of ARXPS, with no

Al_2O_3 observable. We interpret this dramatic change in surface composition as indicative of the unlimited oxide growth reported in the literature [13] for this alloy. The emissivity of this alloy increased linearly from 0.16 to 0.32 over a 7-h heating period.

5. CONCLUSIONS

The objectives of this study were to evaluate dual-wavelength emissivity compensation methods for aluminum alloys subjected to different surface preparations and heating schedules. It was shown that the ISR method is slightly better than the LSR method for all the alloys studied. The ISR method produced the same results as the FOL method since they in fact have the same emissivity compensation requirement. However, different algorithms seemed to work better for different surface conditions. For example, the RWO method worked best for the extruded samples, while the ISR and FOL. methods provided the best results with the cast and saw-cut samples. The temperature errors for any of the methods were still above ± 10 K.

The 1100 series alloys had a constant emissivity for 5 h while being held at a constant temperature of 740 K. This correlated with the fact that Al_2O_3 was the main constituent on the surface of the 1100 series alloys after heating and more importantly that the oxide layer was relatively thin, of the order of 10 nm. The emissivities of the 2224 alloys increased only slightly while heating at a constant 740 K. Although the surface of this alloy, when heated, became greatly enriched in MgO to a depth of roughly 15 nm, Al_2O_3 could still be observed. Thus the surface oxidation showed signs of being limited. The 5052 alloys, on the other hand, were characterized by a rapidly increasing emissivity at a constant temperature. This large change in emissivity appeared to be related to the dramatic restructuring of the alloy surface. Upon heating, the full observation depth, 15 nm, of this alloy became MgO with no Al_2O_3 observed. Thus, the large change in emissivity correlated with the growth of a very thick oxide layer.

From this study, it was determined that the dual-wavelength methods of emissivity compensation do not provide satisfactory performance to achieve ± 3 K for the prescribed temperature and heating schedule conditions. We conclude that the emissivity functions are inappropriate for the behavior of the alloys and that to develop useful dual-wavelength methods, an improved understanding of the spectral emissivity of the materials will be required.

ACKNOWLEDGMENTS

The authors acknowledge the efforts of Mr. A. S. Anderson, Williamson Corporation, for engineering the modifications of the Model 12200 to suit our requirements and for providing valuable advice on experimental procedures and data analysis. Professor D. R. Gaskell, School of Materials Engineering, contributed to developing procedures for appropriate preparation of test samples and our understanding of surface microstructure effects on emissivity. This work was supported in part by the National Science Foundation under Grant CDR 8803017 to the Engineering Research Center for Intelligent Manufacturing Systems, Schools of Engineering, Purdue University. Funding by the Aluminum Company of America, Kaiser Aluminum and Chemicals Corporation, and Inland Steel Company is gratefully acknowledged as well.

REFERENCES

1. M. J. Haugh, in *Theory and Practice of Radiation Thermometry*, D. P. DeWitt and G. D. Nutter, eds. (Wiley, New York, 1988), pp. 905–971.
2. G. M. Foley, *High Temp. High Press.* **10**:391 (1978).
3. D. Y. Svet, *High Temp. High Press.* **4**:715 (1972).
4. M. Watari, Y. Watanabe, S. Chigira, and Y. Tamura, *Yokogawa Tech. Rep.* **29**:25 (1985).
5. T. Andoh, F. D. Banta, T. Kawano, I. Fujimoto, and M. Watari, *Yokogawa Tech. Rep.* **31**:8 (1987).
6. A. S. Anderson, *Proceedings of Aluminum Association Workshop on Sensors*, p. 91 (1986).
7. A. S. Anderson, *Adv. Instrument.* **40**:1337 (1985).
8. B. K. Doloresco, MSME thesis (School of Mechanical Engineering, Purdue University, Lafayette, Ind., August 1986).
9. G. J. Dail, M. G. Furhman, and D. P. DeWitt, *Proc. Fourth Int. Alum. Extrus. Technol. Semin.* **2**:281 (1988).
10. J. H. Scofield, *J. Electron Spectrosc.* **8**:129 (1976).
11. C. J. Powell, *Surf. Interface Anal.* **7**:263 (1985).
12. E. A. Gulbransen and W. S. Wysong, *J. Phys. Chem.* **51**:1087 (1947).
13. C. N. Cochran and W. C. Sleppy, *J. Electrochem. Soc.* **108**:322 (1961).